

Multibreather solitons in the diffraction managed NLS equation

Panayotis Panayotaros

Departamento de Matemáticas y Mecánica, IIMAS–UNAM, Apartado Postal 20-726, México, DF 01000, Mexico

Received 1 June 2005; received in revised form 13 September 2005; accepted 13 September 2005

Available online 30 September 2005

Communicated by C.R. Doering

Abstract

We study analytically and numerically localized breather solutions in the averaged discrete nonlinear Schrödinger equation (NLS) with diffraction management, a system that models coupled waveguide arrays with periodic diffraction management geometries. Localized breathers can be characterized as constrained critical points of the Hamiltonian of the averaged diffraction managed NLS. In addition to local extrema, we find numerically more general solutions that are saddle points of the constrained Hamiltonian. An interesting class of saddle points are “multi-bump” solutions that are close to superpositions of translates of simpler breathers. In the case of zero residual diffraction and small diffraction management, the existence of multibumps can be shown rigorously by a continuation argument.

© 2005 Elsevier B.V. All rights reserved.

PACS: 42.65.Sf; 45.20.Jj

Keywords: Nonlinear Schrödinger equations; Discrete breathers; Variational methods

1. Introduction

In this Letter we study breather and multi-breather solutions in the averaged diffraction managed NLS equation, a lattice system describing optical signals in an array of coupled waveguides with the zigzag geometry introduced in [11]. Our starting point is the parametrically forced (nonautonomous) discrete NLS model proposed by [4] and we study breather solutions in an approximate autonomous discrete system derived by an asymptotic averaging argument. The averaged system provides a good approximation to the original model of [4] and is also of independent interest since it describes an infinite-range nonlinear coupling between lattice sites.

Localized breather solutions of the averaged diffraction managed NLS system are spatially decaying periodic orbits of a special form that can be also characterized as critical points of the Hamiltonian of the averaged system over the set of configuration of constant power. For certain ranges of the parameters the global minima of the constrained variational problem

are attained (see [20]). These extrema correspond to solutions that may be termed ground state or minimal breathers. In the present work we consider more general breathers and also determine their local variational type (i.e. whether they are local extrema or saddles) by examining the Hessian at the critical point. This information is interesting since, by the conservation of the Hamiltonian and the power in the averaged discrete NLS, isolated circles of local extrema are orbitally stable. Also, the iterative numerical methods we used do not appear to use the variational structure of the problem explicitly. The variational type of the numerical solutions must be therefore determined a posteriori.

A first class of numerical solutions that we find are local minima of the Hamiltonian; these are likely to approximate the global minima suggested by the existence argument. Also, we find numerically a variety of other solutions that are saddles of the constrained functional. A special class of such solutions are close to sums of translates of other breather solutions, e.g. of breathers that are local minima. These “multi-bump” breathers are seen for a wide range of parameters, and in the case of zero residual diffraction and small diffraction management their existence is also shown rigorously. These solutions are contin-

E-mail address: panos@mym.iimas.unam.mx (P. Panayotaros).

uations of certain multi-peak solutions of the anti-continuous system, specifically solutions with a $\frac{\pi}{2}$ phase difference between neighboring sites. Related ideas have been used in [5,16]. The proof here relies on the specific form of the nonlinear interaction between the different lattice sites. The argument also applies to higher-dimensional lattices although our numerical study concerns the one-dimensional lattice only. We note that the zero residual diffraction case, while special, is of particular physical importance and in some sense motivates the study of the system.

The Letter is organized as follows. In Section 2 we introduce the averaged equation, review some relevant results on breather solutions, and show the existence of multi-bump breathers for zero residual diffraction. In the third section we describe various types of numerically computed breathers and discuss their variational type.

2. Breather solutions of the averaged equation

We consider the lattice of integers \mathbf{Z} , and complex valued functions $u(t)$ on \mathbf{Z} that evolve according to the nonautonomous system

$$\partial_t u = iD(t)\Delta u - 2i\gamma g(u), \tag{2.1}$$

where

$$(\Delta u)_j = u_{j+1} - 2u_j + u_{j-1}, \quad g_j(u) = |u_j|^2 u_j, \tag{2.2}$$

and f_j is the value of $f : \mathbf{Z} \rightarrow \mathbf{C}$ at the site j . The function D is real valued and γ is a real constant. We further assume that D is T -periodic, and we decompose it as

$$D(t) = \delta + \tilde{d}(t), \quad \text{with } \delta = \frac{1}{T} \int_0^T D(\tau) d\tau \tag{2.3}$$

the average (or residual) diffraction. Physically, t in (2.1) is the distance along the waveguides, while j is the index of the waveguide (see [4,11], also [7,18] for further information on the discrete NLS). Also, u_j is the complex amplitude of (any) one of the components of the electric field at the site j . The initial condition $u(t_0)$ for (2.1) is the emitted light and we may consider initial data at $t_0 = 0$, shifting $D(t)$ if necessary.

In this work we study an averaged version of (2.1). To obtain the averaged equation we first define the new variable a by

$$u(t) = L_t a(t),$$

$$\text{with } L_t = e^{i\tilde{\Lambda}(t)\Delta} \text{ and } \tilde{\Lambda}(t) = \int_0^t \tilde{d}(\tau) d\tau. \tag{2.4}$$

By (2.1) and (2.4), the evolution equation for $a(t)$ is then

$$\partial_t a = i\delta\Delta a - 2i\gamma L_t^{-1} g(L_t a), \tag{2.5}$$

with the initial condition $a(0) = u(0)$. The time dependence is therefore absorbed in the nonlinear term. The averaged equation is then

$$\partial_t a = i\delta\Delta a - 2i\gamma \bar{g}_L(a),$$

$$\text{with } \bar{g}_L(a) = \frac{1}{T} \int_0^T L_\tau^{-1} g(L_\tau a) d\tau. \tag{2.6}$$

Similar averaging arguments have been first used for the continuous version of (2.1), see [3,13].

We consider solutions of (2.5), (2.6) in the space of square-summable complex valued functions on \mathbf{Z} . Specifically, consider the hermitian inner product $\langle u, v \rangle_h = \sum_{n \in \mathbf{Z}} u_n v_n^*$ on pairs of complex valued functions u, v on \mathbf{Z} . We let X be $l_2 = l_2(\mathbf{Z}, \mathbf{C})$, the real Hilbert space of square summable complex valued functions on \mathbf{Z} with the inner product $\langle u, v \rangle = \text{Re}\langle u, v \rangle_h$, $u, v \in X$. Also, $\|u\| = \|u\|_{l_2} = (\langle u, u \rangle)^{\frac{1}{2}}$ denotes the norm of $u \in X$. We also assume that D is piecewise continuous and bounded in $[0, T]$, i.e. has at most a finite number of (finite) jump discontinuities.

As a preliminary step we check that mild solutions of (2.5), (2.6) in X exist for all time; these are continuous, l_2 -valued functions of $t \in \mathbf{R}$ that satisfy the corresponding integral equations. This follows from the Lipschitz continuity of the right-hand sides (uniformly in t) and the fact that the l_2 norm of the solutions of (2.5), (2.6) is conserved. We can furthermore show the following averaging theorem.

Proposition 2.1. *Let $|\gamma|, |\delta| \leq C_1 \varepsilon$, and $\Omega = \frac{2\pi}{T} > C_2$ and consider solutions $a_1(t)$ of (2.5), and $a_2(t)$ of (2.6), corresponding to an initial condition $a_0 \in X$. Then, there exists $\varepsilon_0 > 0$ and constants $C_3, C_4 > 0$ for which $|\varepsilon| \leq \varepsilon_0$ implies*

$$\|a_1(t) - a_2(t)\| \leq C_3 \varepsilon, \quad \forall t \in [0, C_4 \varepsilon^{-1}]. \tag{2.7}$$

Note that the constants C_3, C_4 depend on $C_1, C_2, \|a_0\|$, and ε_0 . The idea is therefore that for T sufficiently small, or equivalently $\frac{|\gamma|}{\Omega}, \frac{|\delta|}{\Omega}$ of $O(\varepsilon)$, ε small, the solutions of (2.5), (2.6) stay $O(\varepsilon)$ close in the l_2 sense over a time interval of $O(\varepsilon^{-1})$. The proof follows from standard averaging arguments. For instance, the Lipschitz continuity in X of right-hand sides, and the local existence theory allow us to apply the arguments of [10] (see also [23, Chapter 3]) to the infinite-dimensional setting.

We now look for nontrivial solutions of (2.6) that have the form $a = e^{-i\lambda t} A$, with $\lambda \in \mathbf{R}$. We refer to these periodic orbits as breathers. Equivalently, by (2.6) breathers are nontrivial functions $A : \mathbf{Z} \rightarrow \mathbf{C}$ that satisfy the equation

$$\lambda A = -\delta\Delta A + 2\gamma \bar{g}_L(A). \tag{2.8}$$

The definition can be augmented by conditions on the behavior of A at infinity. A natural choice here is to consider breathers that also belong to X . This is suggested by the existence theory above, and the variational interpretation of the breather equation (2.8) below.

To see the variational interpretation of (2.8) we let $\|u\|_{l_4}^4 = \sum_{n \in \mathbf{Z}^d} |u_n|^4$ and define the functional \bar{H} on X by

$$\bar{H}(v) = \delta \|D_+ v\|_{l_2}^2 + \gamma \frac{1}{T} \int_0^T \|L_\tau v\|_{l_4}^4 d\tau, \tag{2.9}$$

where $D_+v_j = v_{j+1} - v_j$. Then, the solutions of (2.8) are the critical points of \bar{H} in the set $X_c = \{v \in X: \|v\|_{l_2} = c\}$: we check that the Euler–Lagrange equation corresponding to the constrained variational problem is precisely (2.8). We are here using the fact that $L_t^{-1} = e^{-i\tilde{\Lambda}(t)\Delta} = L_t^\dagger$, the adjoint of L_t in X . Also note that L_t is an isometry, $\forall t$. In [20] we have shown the following:

Theorem 2.2. *Consider the functional \bar{H} above with $\delta \geq 0$ and $\gamma < 0$. Assume that (i) D is piecewise continuous, and (ii) that given $c > 0$, there exists $\mu > 0$ for which $\frac{|\gamma|}{\delta} > \mu$. Then the infimum of \bar{H} on X_c is attained. Furthermore, let $\tilde{a} \in X_c$ satisfy $\bar{H}(\tilde{a}) = \inf_{v \in X_c} \bar{H}(v)$. Then there exists $\lambda \in \mathbf{R}$ for which $A = \tilde{a}$ satisfies (2.8).*

Remark 2.2.1. The constant μ depends on the function \tilde{d} , and c . The sign, and relative size assumptions on δ, γ imply that, given any $c > 0$, the infimum of \bar{H} on X_c is strictly negative. This property is crucial for the proof since otherwise the infimum is not attained. Analogous results on suprema hold for $\delta \leq 0, \gamma > 0$ (see [20]).

Note that \bar{H} and the l_2 norm are invariant under (i) translations in \mathbf{Z} , and (ii) the circle action $v \rightarrow e^{i\phi}v, \phi \in \mathbf{R}$. Thus, if \tilde{a} is a minimizer of \bar{H} on X_c the integer translates of \tilde{a} , and points on the circle $e^{i\phi}\tilde{a}, \phi \in \mathbf{R}$ are also minimizers. Also, for $D \equiv \delta$, i.e. constant, we recover the (local) discrete NLS equation.

A question that is not addressed by Theorem 2.2 is whether the circles of minimizers are isolated sets. The numerical evidence in the next section suggests that this is likely to be the case, at least in the range of parameters examined.

Remark 2.2.2. The problem of finding breather solutions when $\frac{\delta}{\gamma} < 0$ is fixed and c varies, e.g. setting $\gamma = -1$ and fixing $\delta > 0$ is more subtle and for some values of c the infimum of \bar{H} on X_c may fail to be strictly negative. In the case of the (local) discrete NLS it was shown in [24] that if $d \geq 2$ then the infimum of \bar{H} on X_c is strictly negative only if c is above a certain threshold. These results were recently extended to the diffraction managed discrete NLS in [15]. Also, a different variational existence proof where λ is fixed is given in [22].

In the next section we see numerically that in addition to the minimizers, the breather equation has other solutions, some of which are saddles of \bar{H} on X_c . An interesting type of breather solutions are “nonlinear superpositions” of minimizers, i.e. solutions that are close to sums of integer translates of minimizers. More generally, one can also consider analogous nonlinear superpositions of any type of breather solutions. We refer to such “compound” breathers as multi-bump breathers. (The term multi-breathers is used loosely in the literature; here it means critical points that are not local extrema.)

We can describe two simple constructions of multi-bumps for the special cases of (i) the local discrete NLS, and (ii) the diffraction managed discrete NLS with zero average diffraction. In both cases the solutions are obtained by continuation

from solutions of the $D \equiv 0$ limit of the breather equation (2.8). These solutions are also seen numerically in the next section.

For the case (i) of the local discrete NLS, $D \equiv \delta = \text{const}$, we decompose \mathbf{Z} into disjoint sets $U_+, U_-,$ and U_0 , with U_+, U_- finite and consider the local discrete NLS with $\delta = 0, \gamma \neq 0$ (the anti-continuous limit). Then for any λ with $\lambda\gamma > 0$ and any U_+, U_- the corresponding breather equation (2.8) has the solutions $A_j = \pm\sqrt{\frac{\lambda}{2\gamma}}$ for $j \in U_\pm, A_j = 0$ for $j \in U_0$. We denote any such solution by $A(\lambda, U_+, U_-)$. These solutions belong to X_R , the set of real-valued square integrable functions on \mathbf{Z} . X_R is clearly a subspace of X . We have the following:

Proposition 2.3. *Consider λ, γ with $\lambda\gamma > 0$, and a solution $A(\lambda, U_+, U_-)$ of the local discrete breather equation with $\delta = 0$, as above. Then there exists a $\delta_0 > 0$ for which the local discrete breather equation with $|\delta| < \delta_0$ has a unique real solution $A_\delta(\lambda, U_+, U_-) \in X_R$ satisfying*

$$\|A_\delta(\lambda, U_+, U_-) - A(\lambda, U_+, U_-)\| \rightarrow 0 \text{ as } \delta \rightarrow 0. \tag{2.10}$$

Proof. Fix $\lambda, \gamma, \lambda\gamma > 0$ and let $F(\delta, A) = \lambda A + \delta\Delta A - 2\gamma g(A)$ (the dependence on λ is suppressed from the notation). We note that $F(\delta, A) \in X_R$ for $A \in X_R$. We can therefore seek solutions of $F(\delta, A) = 0$ that belong to X_R . The linearization D_2F of F (in X_R) at a solution $\delta = 0, A = A(\lambda, U_+, U_-) \in X_R$ is diagonal in the orthonormal basis $\{\hat{e}(k)\}_{k \in \mathbf{Z}}$ of elements $\hat{e}(k)$ of X_R that vanish outside the site k , specifically the (k, k) diagonal entry of D_2F is λ , if $k \in U_0$, and -2λ , if $k \in U_+ \cup U_-$. The inverse of D_2F therefore exists and is a bounded operator in X_R . It is also easy to check that F and D_2F are continuous in a neighborhood of $(0, A(\lambda, U_+, U_-))$ in $\mathbf{R} \times X_R$. The statement then follows from the implicit function theorem. \square

For small $|\delta|$ we thus have breather solutions that are unique continuations of the breather solutions of the anti-continuous limit breathers. Note that the sign of δ is here irrelevant. A similar argument also applies to the special case (ii) of the dispersion managed breather equation with zero average dispersion. In particular, consider a piecewise continuous T -periodic real function $D(t) = \epsilon\tilde{d}(t)$, with $\int_0^T D(s) ds = 0$ and let $L_t(\epsilon) = e^{i\epsilon\tilde{\Lambda}(t)\Delta}$, with $\tilde{\Lambda}(t) = \int_0^t \tilde{d}(\tau) d\tau$. Also, let

$$\bar{F}(\epsilon, A) = \lambda A - 2\gamma \bar{g}_L(\epsilon)(A) \tag{2.11}$$

with $\bar{g}_L(\epsilon)(A)$ as in (2.6), and $L_\tau = L_\tau(\epsilon), L_\tau^\dagger = L_\tau^\dagger(\epsilon)$. The breather equation (2.8) with $\delta = 0$ and $D(t) = \epsilon\tilde{d}(t)$ is then written as $\bar{F}(\epsilon, A) = 0$ (λ will be fixed and is suppressed from the notation). Defining the subspace

$$Y = \{u \in X: u_{2n} \in \mathbf{R}, u_{2n+1} \in i\mathbf{R}, \forall n \in \mathbf{Z}\} \tag{2.12}$$

we observe that Y is invariant under \bar{F} for all real ϵ and we can therefore try to continue solutions of $\bar{F}(0, A) = 0$ in Y . The invariance of Y is seen by the following:

Lemma 2.4. *The operator $L_t = e^{i\tilde{\Lambda}(t)\Delta}$ of (2.3) is given by*

$$(L_t u)_n = \sum_{m \in \mathbf{Z}} G_t(n - m)u_m, \quad n \in \mathbf{Z}, \tag{2.13}$$

with

$$G_t(k) = e^{-2i\tilde{\Lambda}(t)} (i)^{|k|} \mathcal{J}_{|k|}(2\tilde{\Lambda}(t)), \quad k \in \mathbf{Z}, \quad (2.14)$$

where \mathcal{J}_p is the Bessel function of integer order $p \geq 0$. Moreover, if $A \in Y$ then $\tilde{F}(\epsilon, A) \in Y, \forall \epsilon \in \mathbf{R}$.

Proof. To obtain (2.13) and (2.14) we first calculate the Fourier transform of $L_t u$ and then use the inverse Fourier transform and the definition of the Bessel functions. Details are in [20]. By (2.13) and (2.14) we observe that if $A \in Y$ then $L_t A \in e^{-2i\tilde{\Lambda}(t)} Y, g(L_t A) \in L_t A \in e^{2i\tilde{\Lambda}(t)} Y$ and $L_t^\dagger A \in e^{2i\tilde{\Lambda}(t)} Y$. In $L_t^\dagger g(L_t A)$ the t -dependent global phases then cancel and $L_t^\dagger g(L_t A) \in Y$ for $A \in Y$. Since integration, and multiplication by a real constant also preserve $Y, \tilde{F}(\epsilon, A)$ will also be in $Y, \forall \epsilon \in \mathbf{R}. \square$

As before we decompose \mathbf{Z} into disjoint sets $V_{r,+}, V_{r,-}, V_{i,+}, V_{i,-},$ and $V_0,$ with $V_{r,\pm}, V_{i,\pm}$ finite and consider the discrete NLS with $\epsilon = 0, \gamma \neq 0$ (the anti-continuous limit), and the corresponding local breather equation for some fixed λ satisfying $\lambda\gamma > 0$. Then for any $V_{r,\pm}, V_{i,\pm}$ we have the solutions $A_j = \pm\sqrt{\frac{\lambda}{2\gamma}}$ for $j \in V_{r,\pm}, A_j = \pm i\sqrt{\frac{\lambda}{2\gamma}}$ for $j \in V_{i,\pm}, A_j = 0$ for $j \in V_0$. We denote any such solution by $A(\lambda, V_{r,+}, V_{r,-}, V_{i,+}, V_{i,-})$ and note that it belongs to Y .

Proposition 2.5. Consider λ, γ with $\lambda\gamma < 0,$ and a solution $A(\lambda, V_{r,+}, V_{r,-}, V_{i,+}, V_{i,-})$ of $\tilde{F}(0, A) = 0,$ as above. Then there exists $\epsilon_0 > 0$ for which the breather equation $\tilde{F}(\epsilon, A) = 0$ with $|\epsilon| < \epsilon_0$ has a unique solution $A_\epsilon(\lambda, V_{r,+}, V_{r,-}, V_{i,+}, V_{i,-}) \in Y$ satisfying

$$\|A_\epsilon(\lambda, V_{r,+}, V_{r,-}, V_{i,+}, V_{i,-}) - A(\lambda, V_{r,+}, V_{r,-}, V_{i,+}, V_{i,-})\| \rightarrow 0 \quad \text{as } \epsilon \rightarrow 0. \quad (2.15)$$

Proof. Fix $\lambda, \gamma, \lambda\gamma > 0$ and define $h : X_R \rightarrow Y$ by $h(x_k) = x_k,$ for k even, $h(x_k) = ix_k,$ for k odd. Also define $\tilde{F} : \mathbf{R} \times X_R \rightarrow X_R$ by $\tilde{F}(\epsilon, x) = h^{-1}(\tilde{F}(\epsilon, h(x))),$ i.e. we identify Y with X_R and work with \tilde{F} . The linearization $D_2 \tilde{F}$ of \tilde{F} (in X_R) at a solution $\epsilon = 0, h^{-1}(A(\lambda, V_{r,+}, V_{r,-}, V_{i,+}, V_{i,-})) \in X_R$ is diagonal in the orthonormal basis $\{\hat{e}(k)\}_{k \in \mathbf{Z}}$ of elements $\hat{e}(k)$ of X_R that vanish outside the site $k,$ specifically the (k, k) diagonal entry of $D_2 \tilde{F}$ is $\lambda,$ if $k \in V_0,$ and $-2\lambda,$ if $k \in V_{r,+} \cup V_{r,-} \cup V_{i,+} \cup V_{i,-}$. The inverse of $D_2 \tilde{F}$ therefore exists and is a bounded operator in X_R . To check the regularity properties of \tilde{F} we note that since h is C^1 and Y a subspace of X it is enough to consider the regularity of $F : \mathbf{R} \times X \rightarrow X$ near $(0, A(\lambda, V_{r,+}, V_{r,-}, V_{i,+}, V_{i,-}))$. Letting $B(X)$ be the set of bounded linear operators in $X,$ we note that for any fixed $t \in \mathbf{R}$ the semigroup $L_t(\epsilon) : \mathbf{R} \rightarrow B(X)$ is norm-continuous and hence differentiable in ϵ (see e.g. [12, Chapter 7.1]). The same applies to $L_t^\dagger(\epsilon)$. Also for any fixed $\epsilon \in \mathbf{R}$ the semigroup $L_t(\epsilon) : [0, T] \rightarrow B(X)$ (and similarly $L_t^\dagger(\epsilon)$) is norm-continuous in t in the intervals where D is continuous. With these two observations and the fact that $g : X \rightarrow X$ is C^1 it is routine to check that F and $D_2 F$ are continuous in a neigh-

borhood of $(0, A(\lambda, V_{r,+}, V_{r,-}, V_{i,+}, V_{i,-}))$. The statement then follows from the implicit function theorem. \square

Eqs. (2.1), (2.6) and the breather equation (2.8) can also be considered in the d -dimensional integer lattices \mathbf{Z}^d by letting $\Delta = \sum_{k=1}^d D_{k,+} D_{k,-},$ with $D_{k,+} (D_{k,-})$ the forward (backward) first order difference operators along the k th direction. We also readily generalize the Hilbert space X by considering square summable complex functions on \mathbf{Z}^d . To generalize Proposition 2.3 we work as before with real valued functions on \mathbf{Z}^d . For Proposition 2.5, the analogue of the subspace Y of functions that are invariant under the function \tilde{F} of (2.11) is the set of functions that take real values at sites with coordinates $[n_1, \dots, n_d] \in \mathbf{Z}^d$ that satisfy $n_1 + \dots + n_d$ even, and imaginary values at the remaining sites. This defines a ‘‘checkerboard’’ pattern where the values of neighboring sites have a $\pm \frac{\pi}{2}$ phase difference. The invariance of this subspace of X follows from the d -dimensional expression for L_t in Lemma 2.4 (given in [20]). The proofs of Propositions 2.3, 2.5 then generalize to higher dimensions with minor modifications: in both cases the linearization around the respective multi-peak solutions of the anti-continuous discrete NLS is diagonal and has bounded inverse in the corresponding subspace, while the regularity properties of the breather equation functions are as in $d = 1$.

It is clear that global phase shifts of the solutions discussed above are also solutions. Looking for breathers with prescribed phase differences between neighboring sites had the effect of eliminating the zero eigenvalues obtained by linearizing around the anti-continuous limit multi-peak solutions in the full space X .

3. Numerical breathers and their variational type

To solve the breather equation (2.8) numerically we consider a lattice with N nodes. The starting point is then (2.1) with periodic boundary conditions $u_{j+N+1} = u_j$ and we can repeat the averaging argument above to obtain the periodic analogues of (2.6), and the breather equation (2.8). Further, we approximate the integral in \tilde{g}_L of (2.6) by a finite sum, thus considering the approximate breather equation

$$\lambda A = -\delta \Delta A + 2\gamma \tilde{g}_L(A), \quad \tilde{g}_L(A) = \frac{1}{M} \sum_{m=0}^{M-1} L_{m \frac{T}{M}} g(L_{m \frac{T}{M}}^\dagger A), \quad (3.1)$$

with $A_{j+N+1} = A_j$. The integral was here approximated by the trapezoidal rule for simplicity. The solutions of (3.1) are critical points of

$$\tilde{H}(v) = \delta \sum_{j=0}^{N-1} |(D_+ v)_j|^2 + \frac{\gamma}{M} \sum_{m=0}^{M-1} \sum_{j=0}^{N-1} |(L_{m \frac{T}{M}} v)_j| \quad (3.2)$$

over functions v that satisfy $v_{j+N+1} = v_j$ and $\|v\| = \sum_{j=0}^{N-1} |v_j|^2 = c$ for some $c > 0$. Thus the variational structure of the breather equation is preserved under these approximations. Note that in (3.1), (3.2) the respective dependence of \tilde{g}_L, \tilde{H} on M is suppressed from the notation. We also remark that

Eq. (3.1) is solved numerically with λ fixed. The l_2 norm of the solutions is therefore a priori unknown.

To solve the (3.1) we use Netlib's minpack implementation of Powell's hybrid Newton method (see [17,19]) where we minimize the residual

$$\|A - (\lambda I + \delta \Delta)^{-1} 2\gamma \tilde{g}_L(A)\|. \quad (3.3)$$

We typically accept the result when the residual enters the range 10^{-16} – 10^{-14} . We have also used the Petviashvili iteration (see [3,21])

$$A_{j+1} = \mu_j (\lambda I + \delta \Delta)^{-1} 2\gamma \tilde{g}_L(A_j),$$

$$\text{with } \mu_j = \left| \frac{\langle \tilde{g}_L(A_j), A_j \rangle}{\langle A_j, A_j \rangle} \right|^\sigma, \quad \sigma = \frac{3}{2}, \quad (3.4)$$

where now $\langle u, v \rangle = \sum_{j=0}^{N-1} u_j v_j^*$. The iteration is stopped when $\|A_{n+1} - A_n\|$ and $|\mu_n - 1|$ are to within the range 10^{-16} – 10^{-15} . Note that the frequency λ is always chosen outside the spectrum of $-\delta \Delta$. Also, in each run we increase M until the results become independent of M (to the l_2 accuracies of 10^{-16} – 10^{-15} above). This typically occurs after about $M = 30$.

To determine the local variational type of the numerical breather solutions we consider the Hessian of the constrained functional \tilde{H} at the critical point. If v is a numerical solution of (3.1) for a discretization on N nodes and S the $(2N - 1)$ -sphere in \mathbf{R}^{2N} , the Hessian $\nabla^2 \tilde{H}|_S$ of the restriction of \tilde{H} to S can be computed by first specifying a local coordinate system y around v and then approximating the derivatives $\partial_{y_i y_j} \tilde{H}|_S(v)$ by finite differences. Although we are here using a coordinate-dependent definition of the Hessian, we are interested in intrinsic properties of the Hessian that characterize $\tilde{H}|_S$ near the critical point v . First note that by the phase invariance of \tilde{H} , the Hessian will always have at least one zero eigenvalue that is along the phase symmetry direction. Then, we have that (i) if $\nabla^2 \tilde{H}(v)$ has both positive and negative eigenvalues then v is not a local extremum of \tilde{H} . Also, (ii) if the eigenvalues are nonnegative (nonpositive) and there is only one zero eigenvalue, then v is a local minimum (maximum).

A convenient class of coordinate systems in a neighborhood U of $v \in S$ is obtained by projecting U radially to the tangent hyperplane $v + E$ of S at v and then mapping E to \mathbf{R}^{2N} by choosing an orthonormal basis $\{b_1, \dots, b_{2N-1}\}$ of E . Letting $x \in v + E$ and $F(x) = \tilde{H}(\frac{\|v\|}{\|x\|}x)$, the Hessian $\nabla^2 \tilde{H}|_S(v)$ will be the matrix with entries $\partial_i \partial_j F(v)$, where ∂_i is the partial derivative along the direction of the basis vector b_i . Note that the spectrum of $\nabla^2 \tilde{H}|_S(v)$ is independent of the choice of the orthonormal basis, and only depends on the particular choice of the chart from U to $v + E$. The Hessian is evaluated numerically by replacing the partial derivatives by finite differences, in particular the derivative along a direction b_i is evaluated by centered finite differences using the value of F at points $u \pm hb_i$, $u \pm 2hb_i$, etc. To avoid numerical instability as $h \rightarrow 0$, we use h in a range for which we see agreement between the partial derivatives calculated with finite differences of different orders, and with different h . We typically compare centered difference formulas of $O(h^2)$ and $O(h^4)$ and see that

we can work in the range $h \sim 10^{-7}$ – 10^{-5} . Finally, the eigenvalues of the numerical Hessian are computed using routines from eispack (available at <http://www.netlib.org>, see also [9]).

In the simulations below we have used a diffraction management function

$$D(t) = \begin{cases} \delta + C, & \text{if } t \in [0, \frac{T}{2}); \\ \delta - C, & \text{if } t \in [\frac{T}{2}, T), \end{cases} \quad (3.5)$$

and we vary the parameters $w = \frac{\lambda}{\gamma}$, $\chi = \frac{\delta}{\gamma}$, and $\alpha = \frac{C}{\Omega}$. Equivalently, we set $\gamma = -1$, $\Omega = 1$ and vary δ , and C . In the case $\alpha = 0$ we have the local discrete NLS, while the case $\chi = \alpha = 0$ corresponds to the anti-continuous limit. The results below concern the case $\chi \leq 0$ where, by the previous section, the infimum of \tilde{H} on X_c is attained (for $|\chi|$ sufficiently small). The numerical results we present below were obtained for $N = 128$. Increasing N we obtained practically the same breather solutions with small additional run times. However, the evaluation of the Hessian is computationally expensive and we have used at most $N = 256$ nodes. We argue below that this truncation can give sufficiently accurate results on the spectrum. We have classified the numerical solutions into three types.

Type I. A first type of numerical breathers can be characterized as local minima of the constrained functional \tilde{H} . For $|\chi|$, $|\alpha|$ small these solutions also appear to be continuations of the one-peak breather of the anti-continuous limit. For example, for $\chi \in [-0.1, 0.0]$, $\alpha \in [0.0, 0.4]$, the amplitude of $|A|$ attains its maximum at a single node and decays rapidly to zero. An example is seen in Fig. 1(a). As we increase α , the width of the breather increases, and we eventually see the appearance of two maxima, as in Fig. 2(a). These solutions are symmetric, and their amplitude is concentrated in a set of consecutive nodes. The spectrum of the Hessian for the two examples above are in Figs. 1(b), and 2(b), respectively. In both cases we see one near-zero eigenvalue (less than 4×10^{-3} in absolute value) that we interpret as the zero eigenvalue. The remaining eigenvalues are positive and well separated from zero (larger than 1.25 in Fig. 2(b)). These solutions can be therefore characterized as local minima of \tilde{H} on the constraint and are likely to be periodic approximants of the global extrema of Theorem 2.2. The existence of a clear gap between the zero and smallest positive eigenvalue suggests that the corresponding circles of constrained minimizers are isolated. Moreover, the Peierls–Nabarro barrier for such breathers is nontrivial, and the fact that translates of a minimizer are also minimizers suggests (at least for N finite) the existence of min–max critical points on the constraint. Here, the Peierls–Nabarro barrier is the infimum of the maxima of \tilde{H} over all continuous curves on the constraint that connect a minimal breather to its translate by one site (see also [14] for the local discrete NLS). As we double N we see practically no change in the spectrum of the Hessian. In particular, the new eigenvalues are very near the value 20. A possible explanation is given below. We also note that these solutions were found by both the Powell and Petviashvili algorithms, i.e. both iterations converge to the same solution.

Type II. We have also seen solutions that are also concentrated in a set of consecutive nodes but do not appear to be

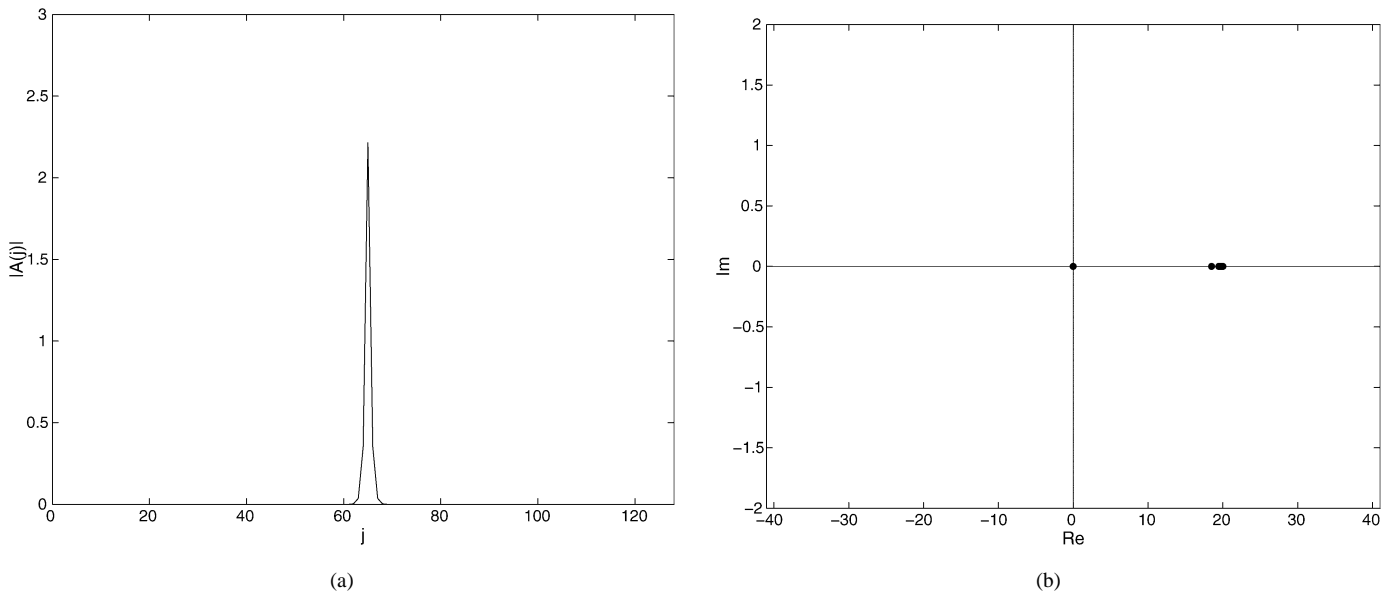


Fig. 1. (a) Breather obtained for $w = -10.0$, $\chi = 0.013$, $\gamma = -1.0$, $A = 0.1$, $\Omega = 1.0$. (b) Hessian of breather in (a). Lowest eigenvalues $r_0 = -0.00012$, $r_1 = 18.4$.

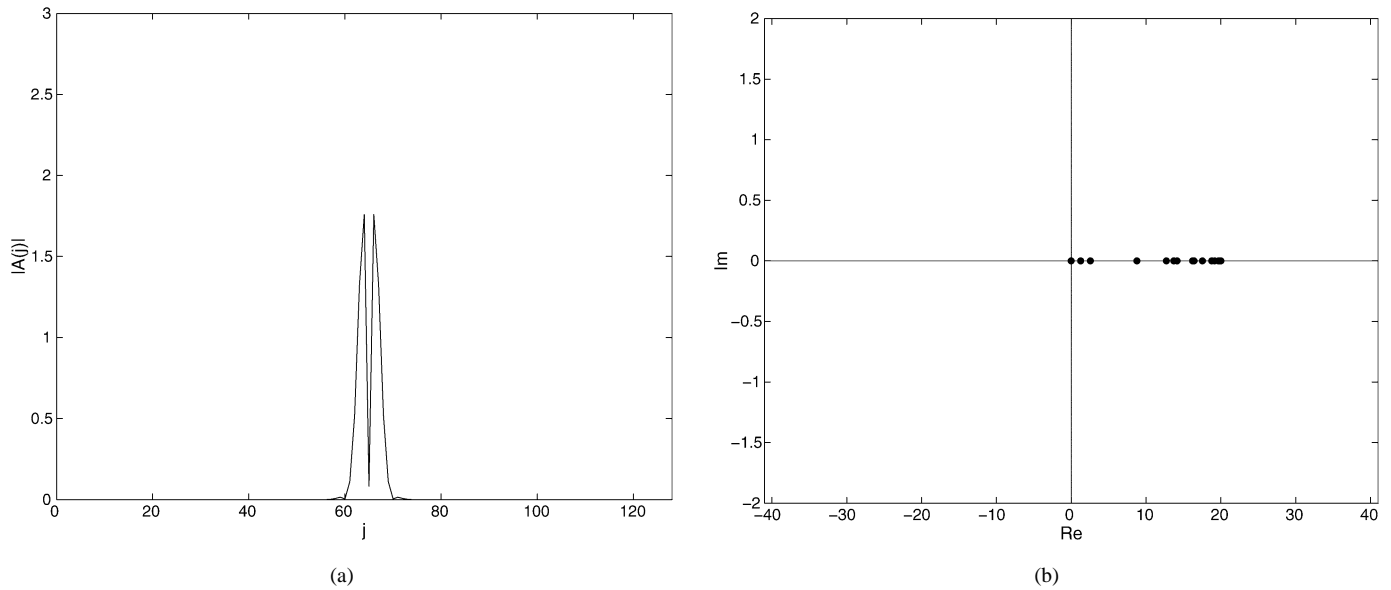


Fig. 2. (a) Breather obtained for $w = -10.0$, $\chi = 0.013$, $\gamma = -1.0$, $A = 0.75$, $\Omega = 1.0$. Same parameters as in Fig. 1(a), except for larger A . (b) Hessian of breather in (a). Lowest eigenvalues $r_0 = -0.0041$, $r_1 = 1.25$.

local extrema of \bar{H} on the constraint. These breathers were seen for larger values of $\alpha \in [0.5, 1.0]$. An example is shown in Fig. 3(a). The main feature of this example is its lack of reflection symmetry and we have also obtained another solution that is the reflection the one shown. Another example is shown in Fig. 4(a). Here we have taken as initial condition two nearby single-peak configurations. The spectrum of the Hessian for the two examples are in Figs. 3(b), 4(b), respectively, and we see clearly the appearance of negative eigenvalues. As in the breathers of the first type, increasing N has the effect of producing eigenvalues that are very near the value 20. The solutions of the second type have been obtained by Powell’s method only.

Type III. A third type of solutions are close to sums of translates of (possibly globally phase-shifted) copies of two

or more of solutions of the two types above. These are multi-bump breather solutions and were also obtained by Powell’s method only. First, setting $\delta = 0$ we see numerically multi-bumps that correspond to the solutions in the subspace Y of Proposition 2.3. An example is shown in Fig. 5(a). In this and other similar examples the initial guess belongs to Y and the iterates stay in Y up to 10^{-7} , i.e. the phase differences between neighboring sites are $\pm \frac{\pi}{2}$ up to 10^{-6} . We have also seen several nonlocal multibump solutions $\delta \neq 0$, $\tilde{d} \neq 0$, i.e. cases not covered by Proposition 2.3. An example is shown in Fig. 6(a). In these more general solutions the amplitude in the regions between the peaks is small, but significantly above the convergence threshold for the residual. To avoid overlap that is too small we have considered translations of at most a few multiples of the rough width of the single breather. As we move away

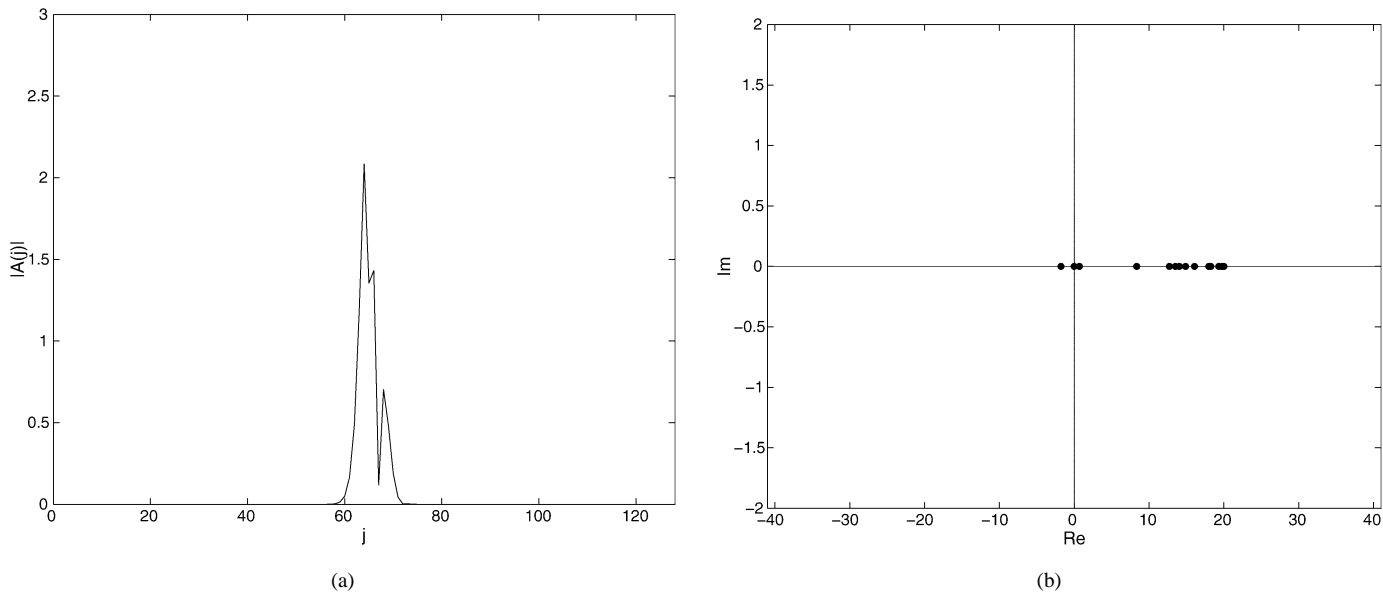


Fig. 3. (a) Breather obtained for $w = -10.0$, $\chi = 0.013$, $\gamma = -1.0$, $A = 0.75$, $\Omega = 1.0$. Asymmetric soliton, same parameters as in Fig. 2(a). (b) Hessian of breather in (a). Lowest eigenvalues $r_0 = -1.76$, $r_1 = -0.0036$, $r_2 = 0.70$.

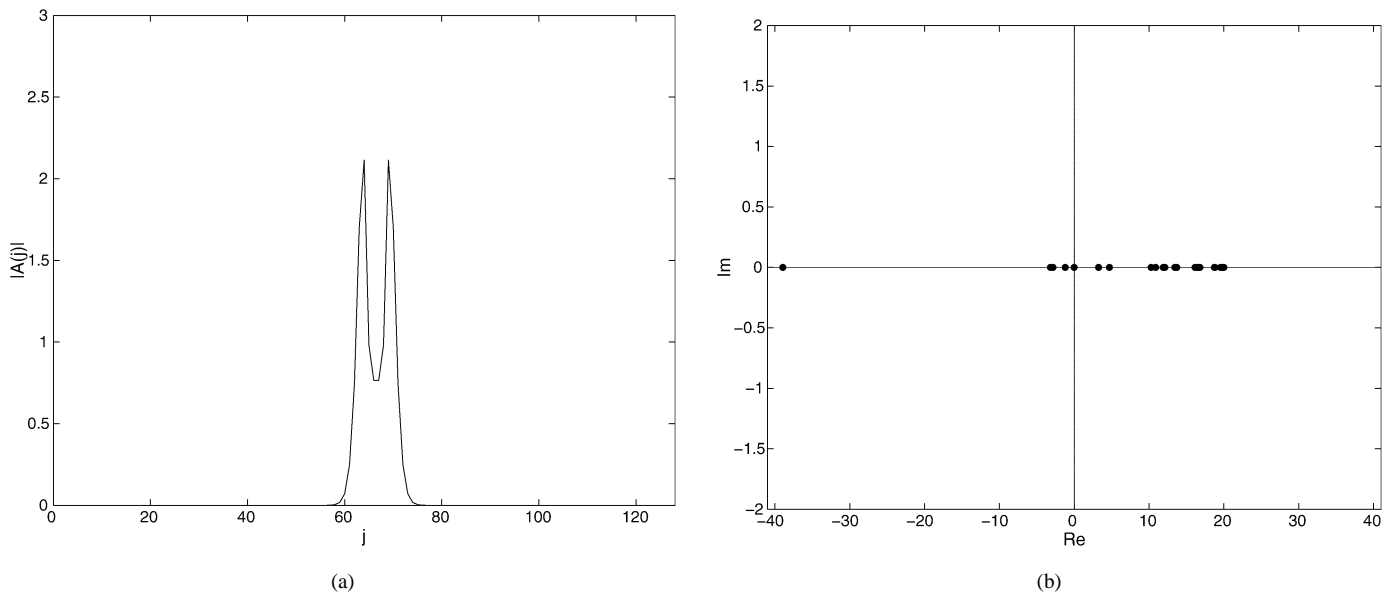


Fig. 4. (a) Breather obtained for $w = -10.0$, $\chi = 0.013$, $\gamma = -1.0$, $A = 0.6$, $\Omega = 1.0$. Twin-peaked breather. (b) Hessian of breather in (a). Lowest eigenvalues $r_0 = -39.9$, $r_1 = -3.18$, $r_2 = -2.84$, $r_3 = -1.19$, $r_4 = -0.0016$, $r_5 = 3.24$.

from $\delta = 0$ the phase difference between neighboring sites moves slowly away from $\frac{\pi}{2}$, for instance for $\chi \in [0.50, 0.55]$ we see phase differences of $\frac{\pi}{2}$ up to 0.06. The corresponding spectra of the Hessian are shown in Figs. 5(b), 6(b). The appearance of negative eigenvalues (near the value -40) indicates that these solutions are not local extrema. Moreover, for $|\chi|, |\alpha|$ sufficiently small, the computed eigenvalues of the Hessian at a n -bump solution seem to follow a simple pattern: there are $n - 1$ negative eigenvalues (near -40), n eigenvalues of small absolute value (one of which should correspond to the zero eigenvalue due to the phase symmetry), while the remaining eigenvalues are positive and accumulate at the value 20. As N is increased we again see that the new eigenvalues will be very near 20.

Remark 3.1. The rationale behind distinguishing the type III solutions is that one could hope to establish their existence by some general argument, e.g. assuming sufficiently large separation between the constituent breathers. This seems more likely for solutions in the subspace Y of (2.12) where we can hope to show the existence of near-superpositions of translates of breathers that are isolated critical points without using the small diffraction management assumption of Proposition 2.5. Some possibly relevant ideas are developed in [1,2,6,8].

Remark 3.2. The version of the Petviashvili algorithm we used could not converge to any of the solutions that are saddle points (i.e. of types II, III). For instance, in the case where we start the iteration at some configuration with several well separated

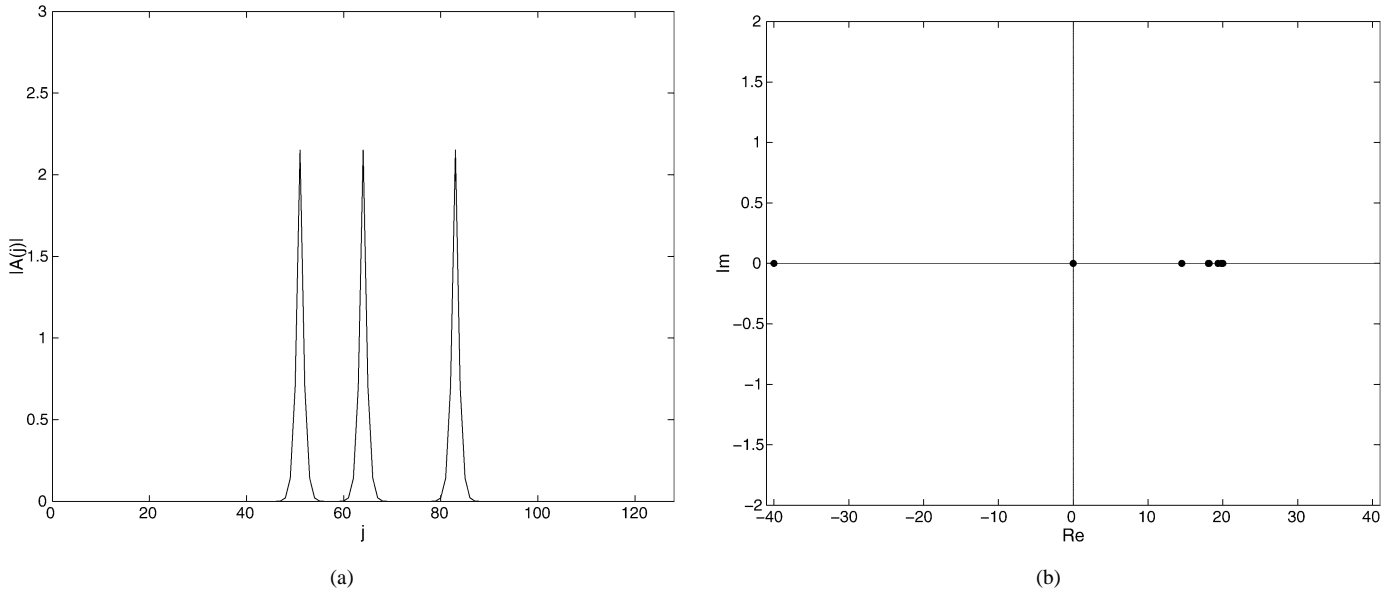


Fig. 5. (a) Breather obtained for $w = -10.0$, $\chi = 0.0$, $\gamma = -1.0$, $A = 0.2$, $\Omega = 1.0$. Three-peaked breather. (b) Hessian of breather in (a). Lowest eigenvalues $r_0 = -40.0$, $r_1 = -39.99$, $r_2 = -0.0011$, $r_3 = 0.0002$, $r_4 = 0.0007$, $r_5 = 14.51$.

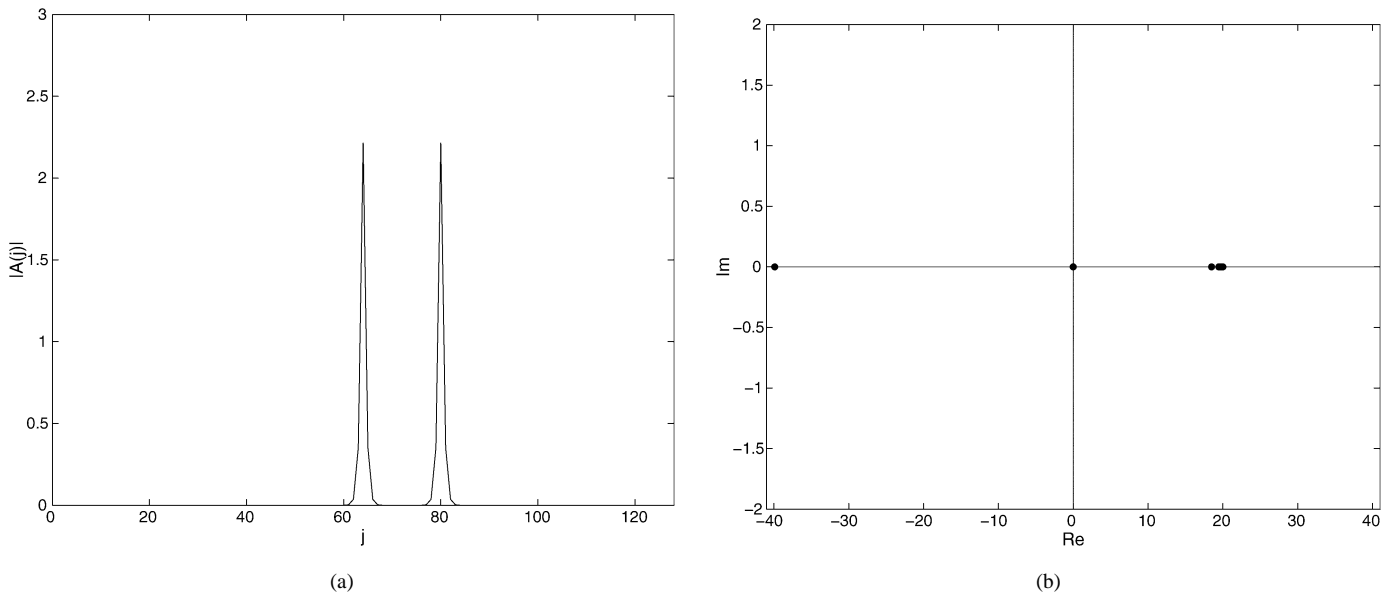


Fig. 6. (a) Breather obtained for $w = -10.0$, $\chi = 0.013$, $\gamma = -1.0$, $A = 0.1$, $\Omega = 1.0$. Two-peak multi-bump breather. (b) Hessian of breather in (a). Lowest eigenvalues $r_0 = -39.9$, $r_1 = -0.00048$, $r_2 = 0.00056$, $r_3 = 18.8$.

peaks the Petviashvili algorithm converges to a solution that is concentrated at one of the peaks.

The observed pattern in the spectrum of the multi-bump solutions (type III) appears to be related to the spectrum of multi-peak breathers of the anti-continuous limit discrete NLS. For these trivial solutions the spectrum of the Hessian can be computed explicitly since we can find a natural basis that makes the matrix diagonal. The basis vectors are normal to the breather v and therefore also form a basis for the tangent hyperplane $v + E$. For instance, set $D \equiv 0$, $\epsilon = 0$, fix λ , γ and consider a breather solution $A(\lambda, V_{r,+}, V_{r,-}, V_{i,+}, V_{i,-}) \in Y$ (in the notation of Proposition 2.5) where the set $V_{r,+} \cup V_{r,-} \cup V_{i,+} \cup V_{i,-}$ consists of n sites (n finite). The Hessian is seen to have a zero

eigenvalue of multiplicity n , an eigenvalue $4\lambda\gamma$ of multiplicity $n - 1$ and an eigenvalue $-2\lambda\gamma$ of infinite multiplicity. The zero eigenvalues are due to the phase symmetry at each peak site, while the $4\lambda\gamma$ eigenvalues correspond to the $n - 1$ vectors that are normal to v and whose components vanish in V_0 . Intuitively, for $\gamma < 0$, moving along these directions makes the configuration more concentrated and decreases \bar{H} . The remaining eigenvalues correspond to the vectors that are zero except at the real or imaginary component of a single site in V_0 . Again, for $\gamma < 0$, moving along these directions makes the configuration less concentrated and increases \bar{H} . A similar conclusion follows for the solutions $A(\lambda, U_+, U_-)$ of Proposition 2.3. In the numerical results shown in the figures we have set $\gamma = -1$, $\lambda = 10$ and as we move away from $\delta = \epsilon = 0$ see that the

infinite multiplicity eigenvalue $-2\lambda\gamma = 20$ now becomes an accumulation point of the spectrum. A possible interpretation of this is that varying δ and ϵ perturbs the Hessian by a compact operator and thus preserves the essential spectrum. The compactness of the operator is probably due to the rapid decay of the breather solutions, i.e. v only changes appreciably at a few sites from its $\delta = \epsilon = 0$ configuration. This scenario is also consistent with the observation that numerical solutions with more nodes only add new eigenvalues near the apparent accumulation point of the spectrum and suggests that the eigenvalues that determine the variational type of the critical point can be computed accurately at least near $\delta = \epsilon = 0$ with a few nodes. It is also interesting that the same accumulation point is present for parameters that are further from the $\delta = \epsilon = 0$ limit; one possibility is that these solutions can be eventually continued to the multi-peak solutions of the anti-continuous limit system.

4. Discussion

We have considered breather and multi-breather solutions for the averaged diffraction managed discrete NLS. The theoretical part of our work used the fact that in the case of zero residual diffraction the breather equation can be solved in the subspace of configurations with a $\frac{\pi}{2}$ phase difference between neighboring sites. This observation allows us to continue trivial multi-peak solutions of the anti-continuous limit to the weakly nonlocal problem and may also be useful far from the trivial limit. The existence of multibump solutions for nonzero average diffraction is an interesting open problem. Numerically, we can find a wider class of breather solutions. Their variational type can be determined by calculating the spectrum of the Hessian on the constraint. For example, in the case of local minima the size of the spectral gap gives us a rough idea of the size of the Peierls–Nabarro barrier. Several features of the spectrum of the Hessian can be also understood qualitatively by considering the anti-continuous limit. A corresponding rigorous perturbation result would also be of interest.

Acknowledgements

The author would like to acknowledge helpful discussions with A. Minzoni, A. Olvera, and P. Padilla.

References

- [1] N. Ackermann, A nonlinear superposition principle and multibump solutions of periodic Schrödinger equations, preprint, 2004.
- [2] S. Angenent, The shadowing lemma for elliptic PDE, in: S.N. Chow, J. Hale (Eds.), *Dynamics of Infinite-Dimensional Systems*, Springer-Verlag, New York, 1987.
- [3] M.R. Ablowitz, G. Biondini, *Opt. Lett.* 23 (1998) 1668.
- [4] M.R. Ablowitz, Z.H. Musslimani, *Phys. Rev. Lett.* 87 (2001) 254102.
- [5] D. Bambusi, *Nonlinearity* 9 (1996) 433.
- [6] V. Coti Zelati, I. Ekeland, E. Séré, *Math. Ann.* 288 (1990) 133.
- [7] D.N. Christodoulides, R.I. Joseph, *Opt. Lett.* 13 (1988) 794.
- [8] V. Coti Zelati, P.H. Rabinowitz, *Commun. Pure Appl. Math.* 45 (1992) 1217.
- [9] J.J. Dongarra, C.B. Moler, Eispack, a package for solving eigenvalue problems, in: W.J. Cowell (Ed.), *Sources and Development of Mathematical Software*, Prentice-Hall, New York, 1984.
- [10] W. Eckhaus, *J. Math. Anal. Appl.* 49 (1975) 575.
- [11] H.S. Eisenberg, Y. Silberberg, R. Morandotti, J.S. Aitchison, *Phys. Rev. Lett.* 85 (2000) 1863.
- [12] H.O. Fattorini, *The Cauchy Problem*, Addison–Wesley, London, 1983.
- [13] I.R. Gabitov, S.K. Turysin, *Opt. Lett.* 21 (1996) 327.
- [14] Y.S. Kivshar, D.K. Campbell, *Phys. Rev. E* 48 (1993) 3077.
- [15] J.T. Moeser, *Nonlinearity* 18 (2005) 2275.
- [16] R.S. MacKay, S. Aubry, *Nonlinearity* 7 (1994) 1623.
- [17] J.J. Moré, D.C. Sorensen, B.S. Garbow, K.E. Hillstom, The minpack project, in: W.J. Cowell (Ed.), *Sources and Development of Mathematical Software*, Prentice-Hall, New York, 1984.
- [18] R. Morandotti, U. Peschel, J.S. Aitchison, H.S. Eisenberg, Y. Silberberg, *Phys. Rev. Lett.* 83 (1999) 2726.
- [19] M.J.D. Powell, A hybrid method for nonlinear equations, in: P. Rabinowitz (Ed.), *Numerical Methods for Nonlinear Algebraic Equations*, Gordon and Breach, New York, 1970.
- [20] P. Panayotaros, *Physica D* 206 (2005) 213.
- [21] V.I. Petviashvili, *Plasma Phys.* 2 (1976) 469.
- [22] A. Pankov, N. Zakharchenko, *Acta Appl. Math.* 65 (2001) 295.
- [23] J.A. Sanders, F. Verhulst, *Averaging Methods in Nonlinear Dynamical Systems*, Springer-Verlag, New York, 1985.
- [24] M.I. Weinstein, *Nonlinearity* 12 (1999) 673.